Received: 24 April 2018 | Revised: 28 August 2018 | Accepted: 7 September 2018

DOI: 10.1002/htj.21379

ORIGINAL ARTICLE

WILEY

Performance effect on the TEG system for waste heat recovery in automobiles using ZnO and SiO_2 nanofluid coolants

Dhruv Raj Karana | **Rashmi Rekha Sahoo**

Department of Mechanical Engineering, Indian Institute of Technology (BHU), Varanasi UP-221005, India

Correspondence
Rashmi Rekha Sahoo, Department of Mechanical Engineering, Indian Institute of Technology (BHU), Varanasi, India.
Email: rrsahoo.mec@itbhu.ac.in

Abstract

Enhancement in heat transfer of the cold side is vital to amplify the performance of a thermoelectric generator (TEG). With enriched thermophysical properties of nanofluids, significant improvement in heat transfer process can be obtained. The current study concerns the performance comparison of an automobile waste heat recovery system with EG-water (EG-W) mixture, ZnO, and SiO_2 nanofluid as coolants for the TEG system. The effects on performance parameters, that is, circuit voltage, conversion efficiency, and output power with exhaust inlet temperature, the total area of TEG, Reynolds number, and particle concentration of nanofluids for the TEG system have been investigated. A detailed performance analysis revealed an increase in voltage, power output, and conversion efficiency of the TEG system with SiO_2 nanofluid, followed by ZnO and EG-W coolants. The electric power and conversion efficiency for SiO_2 nanofluid at an exhaust inlet temperature of 500K were enhanced by 11.80% and 11.39% respectively, in comparison with EG-W coolants. Moreover, the model speculates that an optimal total area of TEGs exists for the maximum power output of the system. With SiO_2 nanofluid as a coolant, the total area of TEGs can be diminished by up to 34% as compared with EG-W, which brings significant convenience for the placement of TEGs and reduces the cost of the TEG system.

KEYWORDS
circuit voltage, conversion efficiency, nanofluid, Reynolds number, thermoelectric generator (TEG), waste heat recovery

1 | INTRODUCTION

The internal combustion engine has a modicum efficiency of around 30 percent.[1] A major component of this energy is wasted in the form of heat from the exhaust gas. Numerous studies[1–3] have been done to recover part of this waste heat by using the thermoelectric generator (TEG). The TEG is a solid-state energy converting device, which produces voltage when the temperature difference is applied across its ends. The absence of moving parts, long service life[4] and compact built makes it a reliable device for converting heat to electricity. Despite its advantages, its large-scale use is subdued by its low efficiency. But TEG is still regarded as an environment-friendly device for waste heat harvesting. The performance of a TEG depends on several factors, that is, material selection, temperature difference, hot-side and cold-side heat transfer, and so on. Development under each of these has rendered an improvement in overall efficiency of TEGs and made them competent with other waste heat recovery methods.

Widespread research on TEG is being done to improve its figure of merit (ZT), which is a measure of its efficiency. The two most important parameters governing the figure of merit, ZT are the thermal conductivity and power factor of the material. Although the two parameters are interdependent, they are in conflict with each other. The various materials used for power generation within 500 to 900 K are Bi_2Te_3, PbTe, PbSe, SnTe, and so on.[5] The most common material used for waste heat recovery applications is bismuth telluride (Bi_2Te_3) because its operating temperature coincides with a temperature of typical automobile exhaust. Bi_2Te_3 composition is uniform and the figure of merit remains more or less constant (~1) within the operating range. This is also because carrier concentration and hence properties can be fine-tuned by alloying it with other alloys like antimony telluride (Sb_2Te_3).[5] It is observed that enhancement of the Seebeck coefficient without a reduction in thermal conductivity often involves the use of heavy metals that are toxic.[6] Rabari et al[7] developed a numerical model evaluating the performance of TEG comprising a p-type nanostructured material of BiSbTe and an n-type Bi_2Te_3 with 0.1 vol.% silicon carbide nanoparticles. Liu et al[8] analyzed the performance on a prototype vehicle and obtained a maximum power of 944 W (1.85% conversion efficiency) during the revolving drum test mode when the temperature difference was 240°C. Another material of practical interest with ZT greater than 1 around 450 to 670 K is Zn_4Sb_3.[9] With the advent of new materials, the challenge still remains to strike a good balance between ZT and the power factor. To further improve in efficiency, segmentation of TEGs have also been developed and the study involved TEG in two configurations: "U shaped" and "multi-pass." It is observed that the efficiency of "multi-pass" was more than twice (3.01%) compared with "U shaped" (1.3%).[10] Studies have also been reported,[11,12] where a combination of heat pipes and TEG is used for waste heat recovery, which was able to produce 10.39 W of power for Bi_2Te_3 and also simulated a unique combined heating cooling and power production (CHCP) unit based on TEG, which runs on waste heat of a 16-kW internal combustion engine. The results showed that the primary energy efficiency of the system was 0.944, while the primary energy and cost saving ratios were 0.304 and 0.417, respectively.

Although extensive research has been done, the nominal efficiency of TEG is a hindrance to its practical application. The nominal efficiency of TEG can be further improved by increasing the temperature difference applied across its end, but there is a practical limit. The efficiency can also be improved by either increasing the heat transfer on the hot side or the cold side.[13,14] It has been found that the cold-side temperature and the cold-side flow rate play crucial roles in the power output of the TEG. Studies have been conducted to enhance the cold-side heat transfer of TEG using traditional coolants like water.[15] But there is a need to search for a new class of coolants with better heat transfer capabilities. Nanofluids seem to be an excellent choice as coolants. Various experiments have been conducted. Nanofluids have higher thermal conductivity than conventional heat transfer fluids like ethylene glycol and water. Nanofluids, on the other hand, offer higher thermal conductivity than base fluids because of the presence of metal oxides. Because of improved thermophysical properties, nanofluids have been extensively used for waste heat recovery of automobiles.[16,17] Yi et al[18] studied the performance of a TEG system with a graphene-water nanofluid as a coolant for cold-side heat transfer and reported an increase of 11.29%, 21.55% and 3.5% in the voltage, power output, and conversion efficiency respectively, with 5% vol. concentration. Also, a similar performance analysis reported an increase in output power by 12.65%, with the use of Cu-EG nanofluid and Cu-EG/W nanofluid.[19]

Large-scale experimentation has been done for various oxide nanofluids. Xie et al[20] concluded that, among all the various samples, EG-MgO nanofluid possess a higher thermal conductivity of 40.6% and low viscosity at 5% vol. concentration. Also, it has been observed that thermal conductivity dropped up to 5% of the initial value when nanofluid was kept for 24 hours, which indicates its stability. The enhanced thermal transport properties of the EG-MgO nanofluid are because of nanoparticle interactions and its lower viscosity.[21] MgO nanoparticles with water and propylene glycol as base fluids have also shown improved heat transfer properties.[22,23] Most of the studies use Maxwell's equations for predicting thermal conductivity. At lower concentration, the model holds true but an anomaly was seen at higher concentrations of the nanofluid[24,25] and it was concluded that the anomaly was due to different particle size, particle clustering, nano layering, and Brownian motions, which are neglected in Maxwell equations. The effect of particle shape on the thermal conductivity and viscosity of ZnO nanofluid at 5% vol. fraction results in an increase of 12%, 14% in thermal conductivity for spherical ZnO nanoparticles, with the particle size between 18 to 23 nm by using ZnO-EG nanofluid for the heat pipe.[26,27] Apart from thermal properties in base fluids, MgO nanostructures have been investigated for antibacterial properties,[28] and the optical properties of ZnO, especially core-shell structures, are under intensive research.[29] Assael et al[30] while working with carbon nanotubes (CNT) and water reported a 34% increase in thermal conductivity at 0.6% volume fraction. Lee et al[31,32] studied the effect of particle concentration with CuO, Al_2O_3 nanoparticles with water as base fluid and found 23%, 34%, and 50% increase in thermal conductivity at 5%, 10% and 15% vol. factions, respectively. A similar enhancement was obtained with TiO_2 nanoparticles at 5% concentration with water as the base fluid.[33] It is evident that by an appropriate choice of nanoparticles, particle concentration, particle size, and base fluids, enhancement in thermal conductivity can be tailored. Heat transfer coefficient is a more practical indicator of improved heat, and researchers[34,35] have analyzed that by the employment of nanofluids, heat transfer properties improved and experimentally confirmed significant enhancement in the heat transfer coefficient.

In the present study, a TEG-based waste heat recovery system is studied with EG-water (EG-W) (50/50), ZnO, and SiO_2 nanofluids in EG-W (50/50) base fluid as coolants. The governing equations have been formulated and solved using (EES). Various performance parameters, the temperature distribution of the TEG modules, with different inlet temperatures of exhaust gas, the concentration of nanofluid, mass flow rate variation (Reynolds number), and

the total area of TEGs have been analyzed. A further comparative study analysis between ZnO, SiO_2 nanofluids and EG-W has been discussed for maximum performance and optimum total area of TEG.

2 | MATHEMATICAL MODELING AND SIMULATION

The configuration of the TEG system with Bi_2Te_3 material properties and its dimensions for P and N-type are shown in Table 1. Conservation of energy forms and the basis of the model have been developed with the following assumptions.

- Heat transfer attains a steady state on both sides of TEG.
- Heat rejected from exhaust gas is equal to the heat gained by the hot side of TEG.
- Heat transfer due to thermal radiation is neglected
- The contact resistances between the TEG—exhaust gas and TEG—coolant is neglected.
- Heat transfer in the ducts is neglected

The fluid flow for hot and cold fluid the TEG system is in a parallel configuration. All the TEGs are assumed to be divided into N_x and N_y computational units. The X-direction has N_x rows, which are marked by the letter i [0, N_x], and the Y-direction has N_y rows, marked by the letter j [0, N_y]. On the basis of the above nomenclature, a computing unit can be represented by the coordinates in the same plane as (i, j) as shown in Figure 1.

The governing equations for the heat transfer process using basic laws of thermodynamics are as follows:

$$Q_{i,h} = N_y\left[\alpha_{\mathrm{pn}} I T_{i,h} + k_{\mathrm{pn}}(T_{i,h} - T_{i,l}) - \frac{I^2 R_{\mathrm{pn}}}{2}\right] \tag{1}$$

$$\mathrm{Q}_{i,l} = N_{\mathrm{y}}\left[\alpha_{\mathrm{pn}} \mathrm{I} T_{i,l} + \mathrm{k}_{\mathrm{pn}}(\mathrm{T}_{i,h} - T_{i,l}) + \frac{\mathrm{I}^2 \mathrm{R}_{\mathrm{pn}}}{2}\right]. \tag{2}$$

TABLE 1 Parameters of thermoelectric material

Semiconductor Parameters	Value
Seebeck coefficient of P-type leg	2.037×10^{-4} V/K
Seebeck coefficient of N-type leg	1.721×10^{-4} V/K
Resistivity of P-type leg	1.314×10^{-5}Ωm
Resistivity of N-type leg	1.119×10^{-5}Ωm
Length of P- and N-type leg	5 mm
Width of P- and N-type leg	5 mm
Height of P- and N-type leg	5 mm
Thermal conductivity of P-type leg	1.265 W/m K
Thermal conductivity of N-type leg	1.011 W/m K

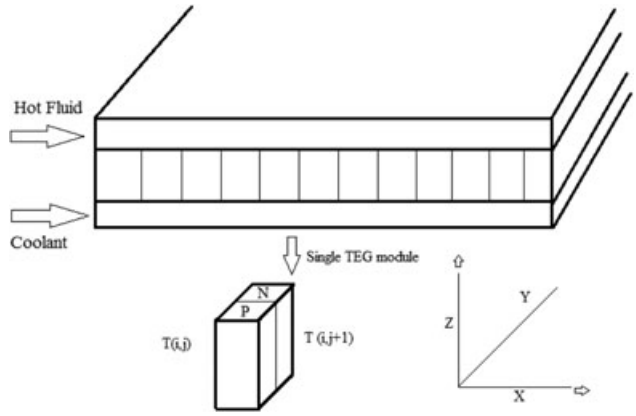

FIGURE 1 Mathematical model and arrangement of the TEG system. TEG, thermoelectric generator

Equations (1) and (2) were taken into account the Joule effect, the Peltier effect, and the heat conduction loss of TEGs. The various electrical properties of the P-N junction are defined as follows:

$$\alpha_{\mathrm{pn}} = \alpha_{\mathrm{p}} - \alpha_{\mathrm{n}}, \tag{3}$$

where

$$k_{\mathrm{pn}} = \frac{\mathrm{l\,b}(\lambda_{\mathrm{p}} - \lambda_{\mathrm{n}})}{h} \tag{4}$$

$$R_{\mathrm{pn}} = \frac{h(\rho_{\mathrm{p}} - \rho_{\mathrm{n}})}{\mathrm{l\,w}}. \tag{5}$$

Newton cooling law describes the heat flux for the hot and cold side of TEGs by

$$Q_{i,h} = N_{\mathrm{y}} h_f \mathrm{Ar}(T_{i,\,fav} - T_{i,h}) \tag{6}$$

$$Q_{i,l} = N_{\mathrm{y}} h_c \mathrm{Ar}(T_{i,l} - T_{i,\,cav}). \tag{7}$$

Because of the steady-state assumption, the heat gained by the hot side of TEGs $Q_{i,h}$ has to be equal to the heat lost by the exhaust. A similar phenomenon occurs with the cold side of TEGs $Q_{i,l}$ and the coolant. Mathematically,

$$Q_{i,h} = C_{\mathrm{pf}} m_f (T_{i,f} - T_{\mathrm{i+1},f}) \tag{8}$$

$$Q_{i,l} = C_{\mathrm{pc}} m_c (T_{\mathrm{i+1},c} - T_{i,c}). \tag{9}$$

The initial and boundary conditions are

$$T_f^1 = 500\,\mathrm{K} \tag{10}$$

$$T_c^1 = 298 \text{ K}. \tag{11}$$

All the thermoelectric modules in the system are connected in series. Thus, the output voltage provided by all TEGs in a column is given by

$$\mathrm{V}_i = N_\mathrm{y}\alpha_\mathrm{pn}(T_{i,h} - T_{i,l}). \tag{12}$$

The total output voltage of the system thus can be calculated as

$$V_\mathrm{total} = N_y\alpha_\mathrm{pn}\sum_{1}^{N_x}(T_{i,h} - T_{i,l}). \tag{13}$$

Total electrical resistance in the circuit is the addition of resistance of P-N junction and load resistance.

$$R_\mathrm{eq} = N_x N_y R_\mathrm{pn} + R_l. \tag{14}$$

Total current is then given by Ohm's law

$$\mathrm{I}_c = \mathrm{V}_\mathrm{total}/R_\mathrm{eq} \tag{15}$$

The suitable hot-side heat transfer coefficient has been taken as $80\,\mathrm{W\,m^2\,K^{-1}}$.[36] The heat transfer coefficient for cold side of TEGs and nanofluid coolants can be calculated by evaluating the Nusselt number of nanofluid for laminar or turbulent conditions[37]

$$\mathrm{Nu_{nf}(laminar)} = 0.4328\mathrm{Re_{nf}^{0.333}Pr_{nf}^{0.4}}(1 + 11.285\varphi^{0.754}\mathrm{Pe_d^{0.218}}) \tag{16}$$

$$\mathrm{Nu_{nf}(turbulent)} = 0.0059\mathrm{Re_{nf}^{.9238}Pr_{nf}^{.4}}(1 + 7.6286\varphi^{.6886}\mathrm{Pe_d^{.001}}) \tag{17}$$

$$\mathrm{Nu_{nf}} = h\,D/k_\mathrm{nf} \tag{18}$$

$$\rho_\mathrm{nf}C_\mathrm{pnf} = (1{-}\varphi)\rho_f C_\mathrm{pf} + \varphi\rho_d C_\mathrm{pd} \tag{19}$$

$$k_\mathrm{nf} = k_\mathrm{bf}\left[\frac{(k_d + 2\mathrm{k_{bf}}){-}2\varphi(k_\mathrm{bf} - k_d)}{(k_d + 2\mathrm{k_{bf}}){+}\varphi(k_\mathrm{bf} - k_d)}\right] \tag{20}$$

$$\mu_\mathrm{nf} = \frac{\mu_\mathrm{bf}}{(1-\varphi)^{2.5}} \tag{21}$$

$$\rho_\mathrm{nf} = \rho_\mathrm{bf}(1-\varphi) + \rho_d\varphi. \tag{22}$$

The inlet condition of the hot fluid and cold fluids (EG-W, ZnO, and SiO_2 nanofluids) are 500 and 298 K, respectively. The mass flow rate and the other fluid properties are listed in Table 2. Using the above-mentioned conditions, the model was solved using engineering equation solver (EES). The

iterative method shown in Figure 2 has been implemented to find the current I and was used to solve the problem in which an initial current I_o was assumed to obtain the temperature distribution of the TEG system.

Power output, a critical parameter to evaluate the performance of TEG can be calculated as

$$P = \sum_{i}^{N_x} (T_{i,h} - T_{i,l}). \tag{23}$$

Thermoelectric conversion efficiency, an equally important parameter, is defined by the ratio of total power output and heat captured at the hot side of the TEG system.

$$\eta_{\text{convs.}} = \frac{P}{\sum_{0}^{\text{Nx}} (Q_{i,h})} \tag{24}$$

The numerical code has been verified with the theoretical result.[36] With the comparison for temperature gradient of hot- and cold-side fluid of the TEM system, for same geometry and operating conditions ($T_{fi} = 500$ K, $T_{ci} = 298$ K, $m_c = m_a = 0.03$ kg/s, 1% *vol. concentration of nanofluids)*, a similar trend has been observed, and maximum 3% and 2% deviations were observed between the predicted and theoretical data.

3 | RESULTS FOR PERFORMANCE TEG SYSTEM

3.1 | Effect of temperature distribution of coolants

The hot-side and cold-side temperature distributions, voltage, total power output and heat transfer rate of TEGs for various coolants (1% vol. fraction ZnO, SiO_2 nanofluids and EG-W) are shown in Figures 3 and 4. The inlet temperature of the exhaust is 500 K, and the coolant mass flow rate is 0.03 kg/s. A gradual decrease in the hot-side TEG temperature is observed for all coolants, due to continuous heat transfer between the exhaust gas and the hot side of the TEGs. However, for coolants with the same mass flow rate, the SiO_2 nanofluid has a higher cold-side heat transfer coefficient as compared with other coolants, which results in lowering the cold-side temperature of TEGs. Also, the temperature gradient between the hot side and cold side of TEGs for SiO_2 nanofluid is higher and followed by ZnO nanofluid and EG-W. The temperature gradient across TEGs is directly proportional to the power and voltage developed. Thus, from the analysis, it is observed that SiO_2 nanofluid has

TABLE 2 Coolant properties

Parameters	Value
Inlet temperature of cold fluid	298 K
Inlet temperature of hot fluid	500 K
Specific heat capacity of EG-W	3340 J/kg K
Specific heat capacity of exhaust gas	1020 J/kg K
Heat transfer coefficient of exhaust gas	80 W m^2 K^{-1}
Mass flow rate of exhaust gas	0.03 kg/s
Mass flow rate of cold fluid	0.03 kg/s

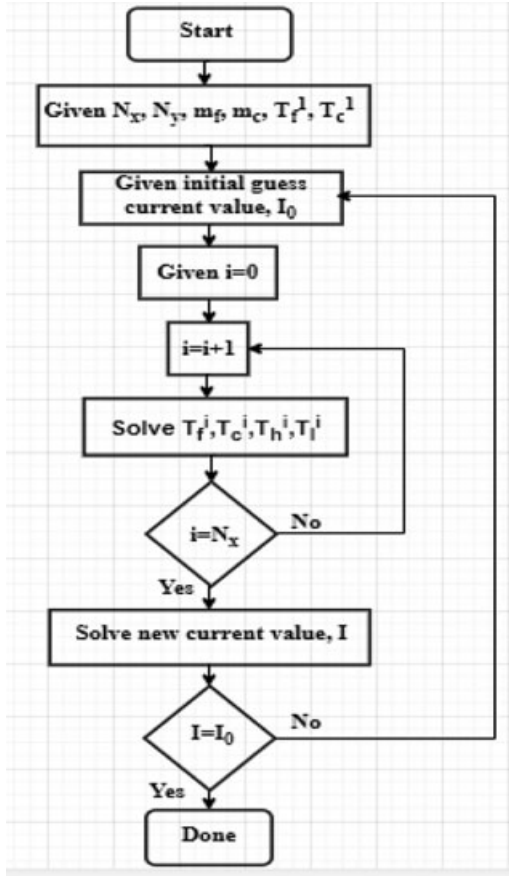

FIGURE 2 Flowchart for iterative calculation

11.80%, 11.39% higher power output, and voltage, respectively, compared with EG-W and followed by ZnO nanofluid and EG-W. However, Figure 5 shows that the heat transfer rate of the hot and the cold side of TEGs gradually decreases for all coolants because of a decrease in temperature difference. It is observed that SiO_2 nanofluid has 1.76% higher heat transfer rate compared with EG-W and followed

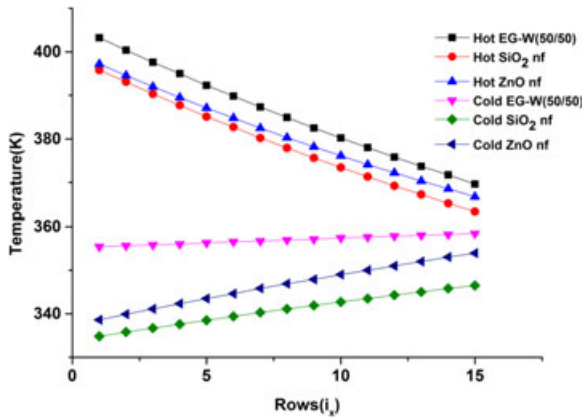

FIGURE 3 Variation of hot- and cold-side temperature of TEMs, thermoelectric material. [Color figure can be viewed at wileyonlinelibrary.com]

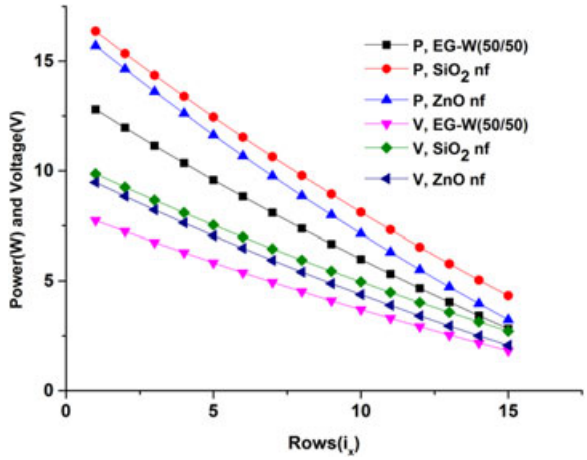

FIGURE 4 Variation of voltage and power of TEMs, thermoelectric material. [Color figure can be viewed at wileyonlinelibrary.com]

by ZnO nanofluid. Therefore, SiO_2 nanofluid as a coolant would yield better performance of TEG amongst all the above-considered coolants.

3.2 | Effect of exhaust inlet temperature

Variations in power output, conversion efficiency and circuit voltage with different exhaust inlet temperatures, for the same mass flow rate of SiO_2, ZnO nanofluids, and EG-W coolants are shown in Figures 6 and 7. It is observed that the power output increases with exhaust inlet temperature for all mentioned coolants. This is because with increasing exhaust inlet temperature, the heat transferred on the hot side of TEGs increases, which results in a higher temperature gradient across TEG modules. It is observed that at an exhaust inlet temperature of 650 K, the increase in power output and voltage for SiO_2 nanofluid are 5.48% and 5.37% respectively, compared with EG-W coolants. The

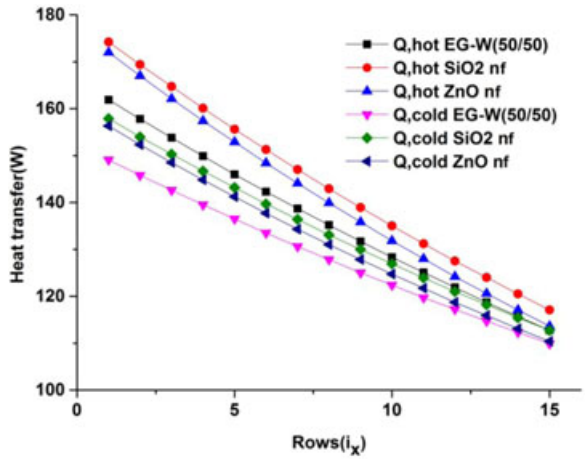

FIGURE 5 Variation of heat transfer rate of TEMs, thermoelectric material. [Color figure can be viewed at wileyonlinelibrary.com]

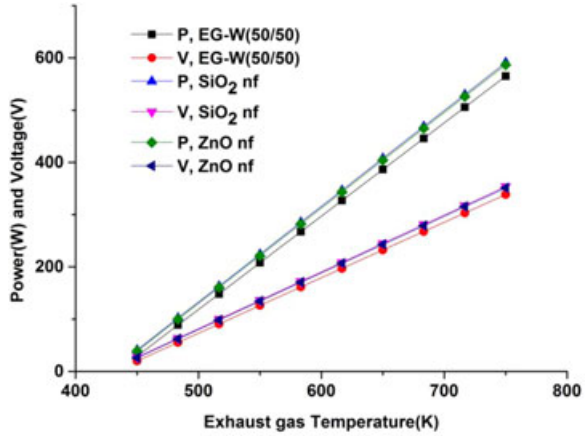

FIGURE 6 Variation of voltage and power for the TEG system [Color figure can be viewed at wileyonlinelibrary.com]

conversion efficiency follows a similar trend, and SiO_2 nanofluid has 3.76% higher conversion efficiency compared with EG-W coolants.

3.3 | Effect of the concentrations of nanofluid

The effects of different concentrations on the power output, circuit voltage, and conversion efficiency performance of the TEG system at exhaust inlet temperature 500 K with a coolant mass flow rate of 0.03 kg/s have been shown in Figures 8 and 9. The present theoretical analysis revealed that power output, conversion efficiency, and circuit voltage for different concentrations of nanofluids are higher than that of EG-W. However, variation in heat transfer with particle volume fraction showed that the performance parameters gradually increase with an increase in the concentration of the nanofluid as shown in Figure 10. Also, SiO_2 nanofluid at 3% vol. fraction has 21.16% higher power output, 0.81% higher conversion

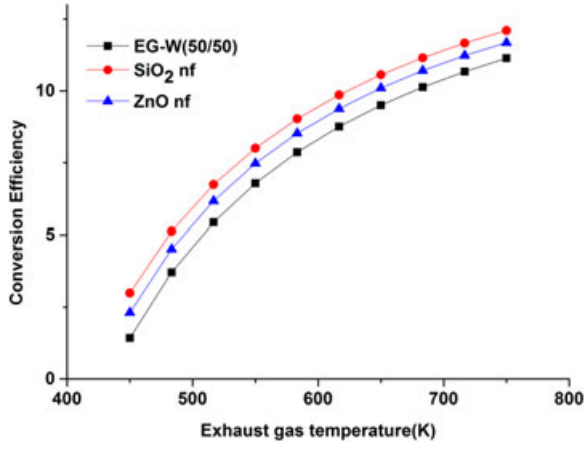

FIGURE 7 Variation of conversion efficiency for the TEG system. [Color figure can be viewed at wileyonlinelibrary.com]

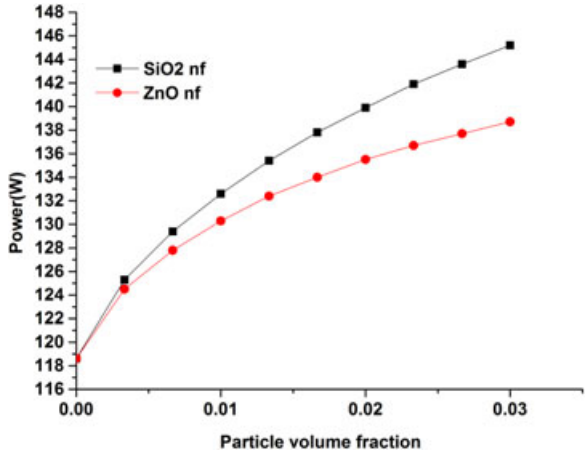

FIGURE 8 Variation of power for the TEG system. [Color figure can be viewed at wileyonlinelibrary.com]

efficiency and 20.33% higher circuit voltage, compared with EG-W coolants and followed by ZnO nanofluid. SiO_2 nanofluid has an enhanced heat transfer coefficient than EG-W, which results in a higher temperature difference with higher performance for the TEG system.

3.4 | Effect of the Reynolds number of the coolants

The distribution of power output, conversion efficiency, and circuit voltage of the TEG system with the Reynolds number (coolant mass flow rate range 0.016-0.1 kg/s) at an inlet exhaust temperature of 500 K and 1% vol. fraction of nanofluids have been shown in Figures 11 and 12 and it has been observed that with an increase in Reynolds number, power output, conversion efficiency, and circuit voltage gradually increase. At a Reynolds number of approximately 2200, SiO_2nanofluid has 3.66% higher power output, 3.62% higher voltage, and 0.22% higher conversion efficiency compared with EG-W coolant and followed by ZnO nanofluid for the TEG system. The possible reason for this may be the enhanced thermal conductivity and the viscosity of the fluid by addition of nanoparticles

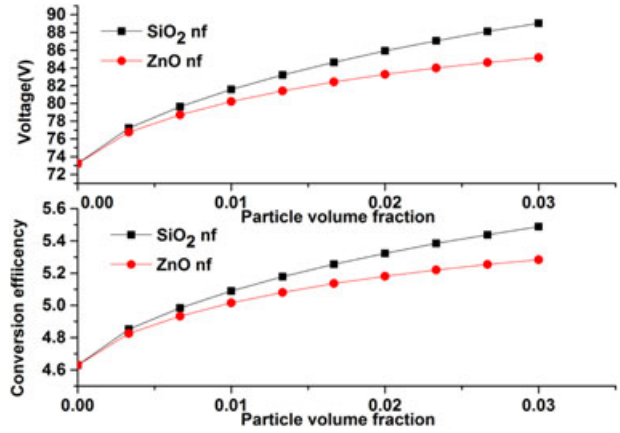

FIGURE 9 Variation of voltage and conversion efficiency for the TEG system. [Color figure can be viewed at wileyonlinelibrary.com]

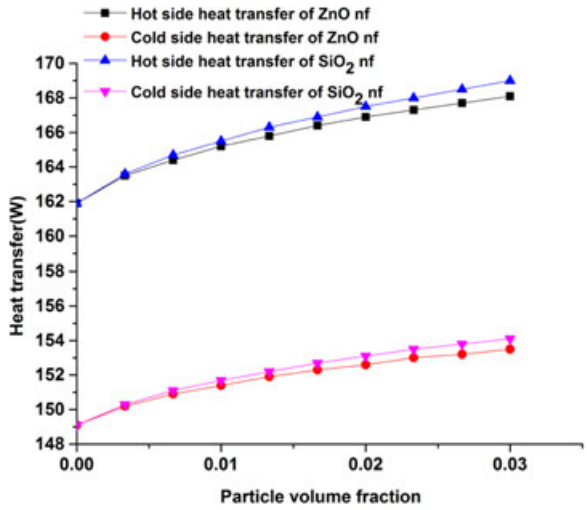

FIGURE 10 Variation of hot and cold-side heat transfer rate of the TEG system. [Color figure can be viewed at wileyonlinelibrary.com]

because of their large aspect ratio. The increase in thermal conductivity results in higher heat transfer, which further results in increased performance of the TEG system.

3.5 | Optimization of total area for power output

The effect on the total area of TEMs with power output has been shown in Figure 13 at an exhaust inlet temperature of 500 K and mass flow rate of exhaust and coolant at 0.03 kg/s. The optimal total area of TEGs exists for the maximum output of the TEG system, which is 0.43 m^2 for EG-W, and 0.2856 and 0.2925 m^2 for SiO_2, ZnO nanofluids respectively, with 1% vol. concentration. Thus, with the application of nanofluid, the optimal area of the TEG system decreases by 33.58% in comparison with EG-W coolants for waste heat recovery through the TEG system. A possible reason is that due to the enhanced heat transfer coefficient by using the nanofluid coolant, the TEGs tend to recover

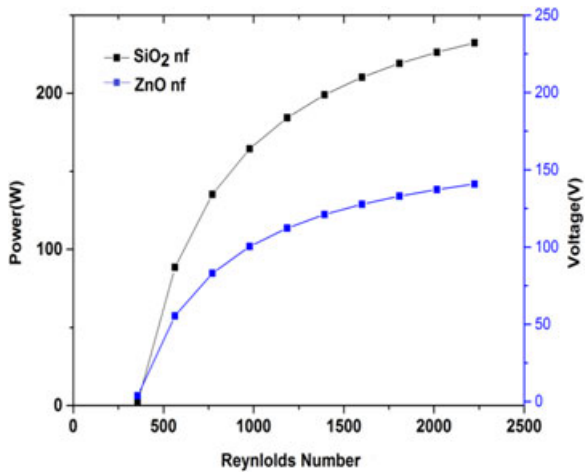

FIGURE 11 Variation of power and voltage of the TEG system. [Color figure can be viewed at wileyonlinelibrary.com]

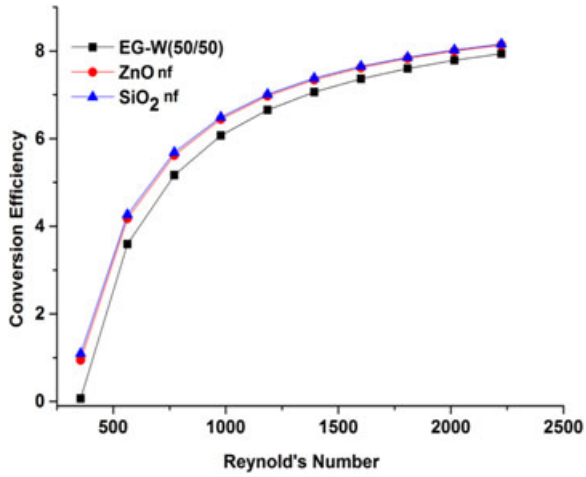

FIGURE 12 Variation of the conversion efficiency of the TEG system. [Color figure can be viewed at wileyonlinelibrary.com]

more waste heat energy as compared with EG-W. Thus, the optimal value of the TEG area shrinks as compared with the EG-W as the coolant. Because of the decrease in total area, a smaller number of TEMs are required to obtain the peak power output. This would result in a lower number of TEGs and their appropriate placement, and thus save the cost of the system. Also, it is observed that for the same total area of the TEG system, the enhancement in power output for the system is approximately 11.8% and 9.86% for SiO_2, ZnO nanofluids, respectively. The enhancement in power output is due to their conductivity and higher heat transfer coefficients.

3.6 | Optimization of the concentration of nanofluid for TEG system

The total power of the TEG system initially increases with the concentration of nanofluids and then declines with a further increase in concentration as shown in Figure 14 and 15. The possible reason is the enhanced heat transfer characteristics with the use of nanofluid initially. However, at higher

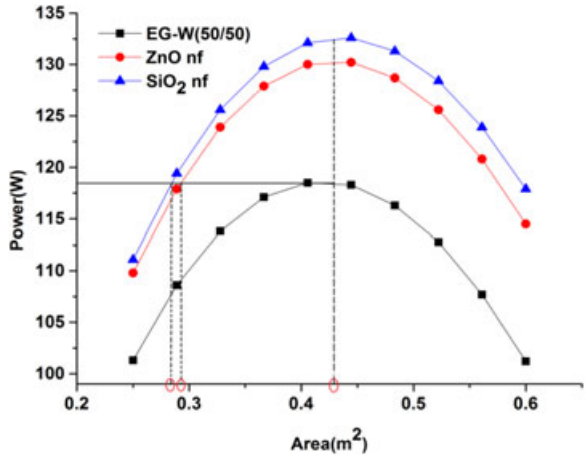

FIGURE 13 Variation of power with the total area of the TEG system. [Color figure can be viewed at wileyonlinelibrary.com]

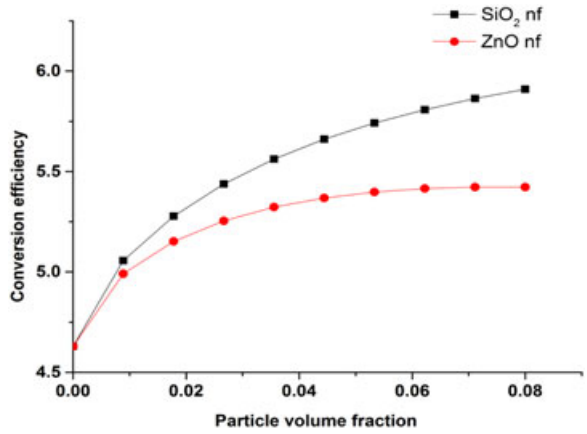

FIGURE 14 Variation of conversion efficiency of the TEG system with vol. fraction of nanofluid. [Color figure can be viewed at wileyonlinelibrary.com]

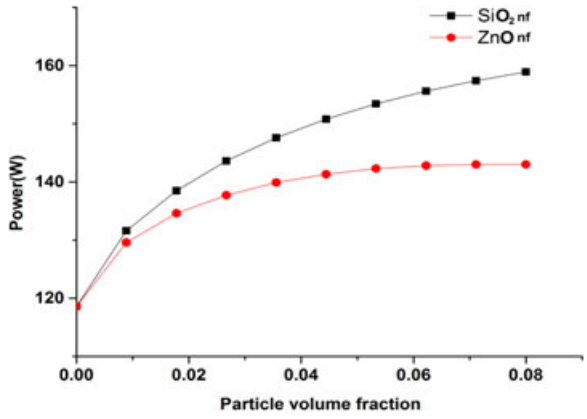

FIGURE 15 Variation of the power output of the TEG system with vol. fraction of nanofluid. [Color figure can be viewed at wileyonlinelibrary.com]

concentrations of nanoparticles, the stability of nanofluid is a challenge that needs to be overcome.[38] Because of the above reason, the concentration of SiO_2 is not increased beyond 8% and for ZnO nanofluid, the optimal range is 7%. At this concentration, ZnO and SiO_2 nanofluids obtain optimum conversion efficiencies of 5.42% and 5.864% respectively, for the same total area of the TEG system. This implies that the SiO_2 nanofluid has a higher upper limit concentration for the output of the TEG system, and hence an important conclusion that can be made that only within a narrow range increasing concentration of nanofluids can improve output performance of the TEG system. Beyond that, the performance deteriorates and thus, the optimum volume concentration is obtained.

4 | CONCLUSIONS

The theoretical analysis presented in this paper investigates and compares the performance of TEG-based waste heat recovery system with EG-W (50/50), SiO_2 and ZnO nanofluids as coolants. The following conclusions have been summarized.

- Compared with EG-W, SiO_2 nanofluid coolant attains a lower temperature at the cold side and a wider temperature gradient across TEGs under the same mass flow rate condition, which effectively improves the power output, conversion efficiency, and circuit voltage of the TEG system.
- For the same area of the TEG system, the power output is enhanced by 11.80% and 9.86% for SiO_2 and ZnO nanofluids in comparison with EG-W coolant.
- Among all the mentioned nanofluids, for the same power output of the TEG system, the optimal total area of TEGs decreases up to 33% for SiO_2 nanofluid as compared with EG-W and followed by ZnO nanofluid. Reduction in the TEG system area will also lead to a reduction in the cost of the overall TEG system.
- The conversion efficiency and circuit voltage for SiO_2 nanofluid increase by 0.9% and 2.83% respectively, for same power output and fixed area of the TEG system, as compared to EG-W and followed by ZnO nanofluid as coolants for the TEG system.
- The optimal concentration of ZnO nanofluid coolant is approximately 7% with 20.57% enhancement in power for the same area of the TEG system.

NOMENCLATURE

Ar	Area of TEG
b	Width of TEG module
C_{pf}	Specific heat capacity of exhaust gas
C_{pc}	Specific heat capacity of coolant
C_{pnf}	Specific heat capacity of nanofluid
h	Height of TEG module
h_c	Heat transfer coefficient for cold side
h_f	Heat transfer coefficient for hot side
I	Current
I_o	Initial current
k_{pn}	Electrical conductivity of P-N junction
l	Length of TEG module
m_c	Mass flow rate of coolant
m_f	Mass flow rate of exhaust gas
$\mathrm{Nu}_{\mathrm{nf}}$	Nusselt number of nanofluid
N_x	Number of TEG module in X direction
N_y	Number of TEG module in Y direction
P	Power output
Pe_c	Peclet number of nanoparticle
$\mathrm{Pr}_{\mathrm{nf}}$	Prandlt number of nanofluid
Q_h^i	Heat transfer per unit area from hot side
Q_l^i	Heat transfer per unit area from cold side
R_{eq}	Total resistance of the TEG modules
$\mathrm{Re}_{\mathrm{nf}}$	Reynold number of nanofluid
R_l	Load resistance
R_{pn}	Resistance of P-N junction
T_f^i	Initial exhaust temperature
T_h^i	Temperature of hot side TEG module
T_c^i	Initial coolant temperature

T_l^i Temperature of cold side TEG module
T_{cav}^i Average coolant side temperature
T_{fav}^i Average exhaust side temperature
T_c^{i+1} Exit coolant temperature
T_f^{i+1} Exit exhaust temperature
V_i Discretized voltage of TEG module
V_{total} Voltage for TEG system
α_n Seebeck coefficient for N- type material
α_p Seebeck coefficient for P- type material
λ_n Thermal conductivity of N- type leg
λ_p Thermal conductivity of P- type leg
ρ_{nf} Density of nanofluid
ϕ Volume fraction of nanofluid

ORCID

Rashmi Rekha Sahoo http://orcid.org/0000-0001-5494-8647

REFERENCES

1. Yu C, Chau KT. Thermoelectric automotive waste heat energy recovery using maximum power point tracking. *Energy Convers Manage*. 2009;50:1506-1512.
2. Weng CC, Huang MJ. A simulation study of automotive waste heat recovery using a thermoelectric power generator. *Int J Therm Sci*. 2013;71:302-309.
3. Liu X, Deng YD, Li Z, Su CQ. Performance analysis of a waste heat recovery thermoelectric generation system for automotive application. *Energy Convers Manage*. 2015;90:121-127.
4. Fisk LA. A journey into the unknown beyond. *Science*. 2005;309(5743):2016-2017.
5. Twaha S, Zhu J, Yan Y, Li B. A comprehensive review of thermoelectric technology: materials, applications, modelling and performance improvement. *Renew Sustainable Energy Rev*. 2016;65:698-726.
6. Ohta H, Kim S, Mune Y, et al. Giant thermoelectric Seebeck coefficient of a two-dimensional electron gas in $SrTiO_3$. *Nat Mater*. 2007;6(2):129-134.
7. Rabari R, Mahmud S, Dutta A. Numerical simulation of nanostructured thermoelectric generator considering surface to surrounding convection. *Int Commun Heat Mass Transf*. 2014;56:146-151.
8. Liu X, Deng YD, Li Z, Su CQ. Performance analysis of a waste heat recovery thermoelectric generation system for automotive application. *Energy Convers Manag*. 2015;90:121-127.
9. Snyder GJ, Christensen M, Nishibori E, Caillat T, Iversen BB. Disordered zinc in Zn4Sb3 with phonon-glass and electron-crystal thermoelectric properties. *Nat Mater*. 2004;3(7):458-463.
10. Bensaid S, Brignone M, Ziggiotti A, Specchia S. High efficiency thermoelectric power generator. *Int J Hydrog Energy*. 2012;37(2):1385-1398.
11. Remeli MF, Tan L, Date A, Singh B, Akbarzadeh A. Simultaneous power generation and heat recovery using a heat pipe assisted thermoelectric generatorsystem. *Energy Convers Manag*. 2015;91:110-119.
12. Wang JL, Wu JY, Zheng CY. Simulation and evaluation of a CCHP system with exhaust gas deep-recovery and thermoelectric generator. *Energy Convers Manag*. 2014;86:992-1000.
13. Wang Y, Dai C, Wang S. Theoretical analysis of a thermoelectric generator using exhaust gas of vehicles as heat source. *Appl Energy*. 2013;112:1171-1180.
14. Liu X, Li C, Deng YD, Su CQ. An energy-harvesting system using thermoelectric power generation for automotive application. *Int J Electr PowerEnergy Syst*. 2015;67:510-516.
15. Wang L, Romagnoli A. Cooling system investigation of thermoelectric generator used for marine waste heat recovery. In: IEEE 2nd Annual Southern Power Electronics Conference; 2016, pp. 1-6
16. Senthilraja S, Karthikeyan M, Gangadevi R. Nanofluid applications in future automobiles: comprehensive review of existing data. *Nano-Micro Lett*. 2010;2(4):306-310.

17. Sidik NAC, Yazid MNAWM, Mamat R. A review on the application of nanofluids in vehicle engine cooling system. *Int Commun Heat Mass Transf*. 2015;68:85-90.
18. Li Y, Wu Z, Xie H, et al. Study on the performance of TEG with heat transfer enhancement using graphene-water nanofluid for a TEG cooling system. *Sci China Tech Sci*. 2017;60(No.8):1168-1174.
19. Li Z, Li W, Chen Z. Performance analysis of thermoelectric based automotive waste heat recovery system with nanofluid coolant. *Energies*. 2017;10(1489):1-15.
20. Xie H, Yu W, Chen W. MgO nanofluids: higher thermal conductivity and lower viscosity among ethylene glycol-based nanofluids containing oxide nanoparticles. *J Exp Nanosci*. 2010;5(5):463-472.
21. Yu W, Xie HQ, Li Y, Chen LF. The thermal transport properties of ethylene glycol based MGO nanofluids. In: ASME 2009 7th International Conference on Nanochannels, Microchannels, and Minichannels; 2009. pp. 901-905
22. Shoghl SN, Jamali J, Moraveji MK. Electrical conductivity, viscosity, and density of different nanofluids: an experimental study. *Exp Therm Fluid Sci*. 2016;74:339-346.
23. Manikandan S, Rajan KS. Rapid synthesis of MgO nanoparticles and their utilization for formulation of a propylene glycol based nanofluid with superior transport properties. *RSC Adv*. 2014;4(93):51830-51837.
24. Maxwell JC. *A Treatise on Electricity and Magnetism*. Cambridge, UK: Oxford University Press; 1904:435-441.
25. Jang SP, Choi SUS. Role of Brownian motion in the enhanced thermal conductivity of nanofluids. *Appl Phys Lett*. 2004;84:4316-4318.
26. Jeong J, Li C, Kwon Y, Lee J, Kim SH, Yun R. Particle shape effect on the viscosity and thermal conductivity of ZnOnanofluids. *Int J Refrig*. 2013;36:2233-2241.
27. Saleh R, Putra N, Prakoso SP, Septiadi WN. Experimental investigation of thermal conductivity and heat pipe thermal performance of ZnO nanofluids. *Int J Therm Sci*. 2013;63:125-132.
28. Bindhu MR, Umadevi M, Micheal MK, Arasu MV, Dhabi NAA. Structural, morphological and optical properties of MgO nanoparticles for antibacterial applications. *Mater Lett*. 2016;166:19-22.
29. Kahouli M, Barhoumi A, Bouzid A, Al-Hajry A, Guermazi S. Review: structural and optical properties of ZnO nanoparticles prepared by direct precipitation method. *Superlattices Microstruct*. 2015;85:7-23.
30. Assael MJ, Metaxa IN, Arvanitidis J, Christofilos D, Lioutas C. Thermal conductivity enhancement in aqueous suspensions ofcarbon multi-walled and double-walled nanotubes in the presenceof two different dispersants. *Int J Thermophys*. 2005;26(3):647-664.
31. Lee S, Choi SUS, Li S, Eastman JA. Measuring thermal conductivity of fluids containing oxide nanoparticles. *J Heat Transfer*. 1999;121:280-289.
32. Xie H, Wang J, Xi T, Liu Y, Ai F. Dependence of the thermalconductivity of nanoparticle-fluid mixture on the base fluid. *J Mater Sci Lett*. 2002;21(19):1469-1471.
33. Murshed SMS, Leong KC, Yang C. Enhanced thermal conductivity of TiO2—water based nanofluids. *Int J ThermSci*. 2005;44(4):367-373.
34. Yang Y, Zhang ZG, EA, Anderson WB, Wu G. Heat transferproperties of nanoparticle-in-fluid dispersions (nanofluids) in laminar flow. *Int J Heat Mass Transfer*. 2005;48:1107-1116.
35. Kulkarni DP, Namburu PK, Ed bargar H, Das DK. Convective heat transferand fluid dynamic characteristics of SiO_2 ethylene glycol/water nanofluid. *Heat Transfer Eng*. 2008;29(12):1027-1035.
36. He W, Wang S, Lu C, Zhang X, Li Y. Influence of different cooling methods on thermoelectric performance of an engine exhaust gas waste heat recovery system. *Appl Energy*. 2016;162:1251-1258.
37. Peyghambarzadeh SM, Hashemabadi SH, Hoseini SM, Seifi jamnani M. Experimental study of heat transfer enhancement using water/ethylene glycol based nanofluids as a new coolant for car radiators. *Int Commun Heat Mass Transf*. 2011;38:1283-1290.
38. Pak BC, Cho YI. Hydrodynamic and heat transfer study of dispersed fluids with submicron metallic oxide particles. *Exp Heat Transf*. 1998;11:151-170.

How to cite this article: Karana DR, Sahoo RR. Performance effect on the TEG system for waste heat recovery in automobiles using ZnO and SiO_2 nanofluid coolants. *Heat Transfer—Asian Res*. 2019;48:216-232. https://doi.org/10.1002/htj.21379